

TRANSPIRATION COOLING OF TWO-DIMENSIONAL
POROUS BODIES USING CHEMICALLY
REACTING AND NONREACTING
COOLANTS

by

ADELL WARREN BRECHEISEN II

B.S., Kansas State University, 1967

A THESIS

submitted in partial fulfillment of the
requirements for the degree

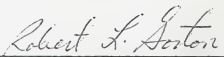
MASTER OF SCIENCE

Department of Mechanical Engineering

KANSAS STATE UNIVERSITY
Manhattan, Kansas

1969

Approved by:


Major Professor

LD
2668
74
1969
B7

TABLE OF CONTENTS

Chapter	Page
I. INTRODUCTION.	1
Mass Transfer Cooling.	1
Transpiration Cooling with Reactive Coolants	4
II. ANALYSIS.	7
Introduction	7
Transpiration Cooling System	7
Turbine Blade Model.	7
Analysis	9
Boundary Conditions.	9
Convection Coefficient	12
Ammonia Dissociation Reaction Rate Equation.	13
Assumptions.	14
Discrete Approximation of the System	15
Results and Discussion	17
III. EXPERIMENT.	24
Introduction	24
Apparatus.	24
Procedure.	30
Results.	31
Conclusions.	36
Interpretation of Experimental Results in Light of Analytical Results	39
IV. SUMMARY	42
REFERENCES.	43
NOMENCLATURE.	45
APPENDICES.	47
Appendix A	48
Appendix B	55
ACKNOWLEDGEMENTS.	58
VITA.	59

LIST OF FIGURES

Figure	Page
1. Transpiration cooling system.	8
2. Streamlined cylinder model.	10
3. Half-model with sample nodal system. Nodes are based on equal distance at the outside surface	11
4. Temperature versus x/L for transpiration cooling with hydrogen and nitrogen (temperatures for outside surface)	19
5. Temperature versus y/L at forward stagnation point for nitrogen and hydrogen.	20
6. Temperature versus x/L at forward stagnation point for ammonia.	21
7. Temperature and fraction of coolant dissociated versus y/L for ammonia (dotted lines are for dissociation). The percent of dissociation for $F = .003$ was too low to plot on this coordinate system.	22
8. Schematic diagram of experimental apparatus	25
9. Iron pipe and test section.	27
10. Porous sample and associated hardware	28
11. Thermocouple locations. The thermocouples were mounted at the center of the cylinder.	32
12. Exterior surface temperature versus θ for 1 1/2 inch cylinder.	34
13. Temperature versus y/L at forward stagnation point for 1 1/2 inch cylinder.	35
14. Temperature versus θ for 1 inch cylinder.	37
15. Temperature versus θ found analytically for 1 1/2 inch cylinder.	41

INTRODUCTION

Mass Transfer Cooling

The problem of maintaining structural integrity of parts subjected to high convective heating rates is of interest in this report. There are two possible causes of high convective heating. The first is viscous dissipation in the boundary layer. This occurs, for example, when a space vehicle reenters the earth's atmosphere. The second is convection heating by high energy fluid streams, such as those encountered by turbine blades or rocket nozzles.

Thermal protection of structures experiencing high convective heating is often necessary to prevent their failure. One way to achieve thermal protection is by application of mass transfer cooling.

Mass transfer cooling involves the displacement of material from a surface in order to protect it from high convective heating. There are three fundamentally different types of mass transfer cooling; (1) ablation, (2) film cooling, and (3) transpiration cooling.

In ablation, the surface of the part to be protected is constructed of a material which undergoes thermal erosion (ablation) at high temperatures. Ablation accomplishes cooling in two ways. First, the ablating surface acts as a heat sink, thus shielding the material underneath from high heating flux. Secondly, the ablation products alter the boundary layer in a manner which reduces heat transfer. Ablation has two major advantages. It requires no auxiliary equipment (pumps, valves, etc.) and it is self regulating, i.e.

higher heating rates increase the rate of ablation. Ablation has two major disadvantages. First, as the surface erodes away, the surface area changes, causing a change in the external flow characteristics. This renders it unsuitable for cooling turbine blades or rocket nozzles where flow passage geometry must be preserved. The second disadvantage is that after the protective surface has eroded away, the structure it was protecting is left vulnerable to severe heating and probable failure. Ablation has been utilized successfully for thermal protection of reentry vehicles and for short duration firing rocket nozzles.

Film cooling involves pumping a fluid coolant through discrete slots in a surface. The coolant forms a film on the surface which protects it from high convective heating. Special emphasis must be placed on the size, shape, and position of the coolant outlets in order to avoid irregularities in the film and to achieve complete filming of the surface. This is necessary to avoid local hot spots. Any irregularities in the film at the injection ports will become enlarged downstream. Film cooling is often used to cool turbine blades and vanes.

Transpiration cooling is accomplished by forcing a coolant fluid through a porous material. Transpiration cooling involves two mechanisms to accomplish thermal protection.

- (1) The pores in the material greatly increase the contact area between the coolant and the matrix, thus increasing the convection cooling of the matrix.
- (2) The injection of the coolant into the boundary layer alters the temperature and velocity distributions in a manner which reduces heat transfer. This is called the "heat blockage" effect.

Heat blockage effects are most pronounced in laminar flow regimes. This

is largely due to the absence of "washing" of the surface which is present in turbulent flows. Washing causes destruction of part of the coolant film on the surface thereby reducing the heat blockage effect. One major disadvantage of transpiration cooling is that it causes large temperature gradients in the porous matrix.

Transpiration cooling requires the same basic equipment as film cooling, the major mechanical difference being the method of coolant injection. Other differences include the coolant distribution over the surface and the internal heat rejection feature of transpiration cooling. Due to the mechanical similarity of film cooling and transpiration cooling, the two are generally applicable to the same types of cooling problems. The major similarities between ablation and transpiration cooling are that they both possess the internal heat rejection feature, although it is accomplished differently in each method, and that they both provide the boundary layer heat blockage effect.

A brief survey of work in the transpiration cooling field prior to 1960 is given by Leadon (1)*. Kelly and L'Ecuyer (2) review the literature pertaining to transpiration cooling and report on the state of the art up to 1966.

Kelly and L'Ecuyer (2) discuss experimental results which indicate that low molecular weight gases are more effective transpiration coolants than gases having relatively high molecular weights. The reason for this has been attributed to more effective heat blockage by the lighter gases. However, gases with low molecular weights tend to have relatively high specific heats, therefore it is also possible to attribute part of their increased effectiveness to greater heat absorption during the period of contact between the coolant and the porous matrix.

*Numbers in parentheses refer to references.

Transpiration Cooling with Reactive Coolants

In order for a gas to be effective as a transpiration coolant, it should be able to fulfill certain desirable requirements. These requirements include maximum heat absorption, maximum heat blockage, oxidation control, and fuel value after entry into the free stream. A coolant which undergoes an endothermic chemical reaction in the temperature ranges of interest (i.e., permissible material temperatures) can theoretically fulfill many of these requirements more efficiently than a nonreacting coolant.

A transpiration coolant absorbs heat as it passes through a porous material. If the coolant is nonreacting, the amount of heat absorbed is proportional to the temperature increase of the coolant, time of contact between coolant and matrix, specific heat of the coolant, and the coolant mass flow rate. If the coolant undergoes an endothermic reaction (e.g., endothermic dissociation) during its contact period with the porous matrix the amount of heat absorbed will be proportional to the reaction rate in addition to the above. Therefore, if all other conditions are equal, a reacting coolant will absorb more heat than a nonreacting coolant.

The products of a dissociation reaction have a lower effective molecular weight than the reactant, resulting in a greater heat blockage effect than would be realized with a nonreacting coolant. The products also will generally have a higher effective specific heat than the reactant. This increases the coolant heat absorption during its contact with the matrix over the heat absorption which would be realized if the specific heats of the products and reactant were equal.

If the dissociation reaction rate is proportional to temperature,

large temperature gradients can be reduced. As the temperature of one portion of the matrix starts to increase, the dissociation rate increases proportionately. This results in the coolant absorbing more heat. With more dissociation occurring, the effective molecular weight of the mixture of coolant and dissociation products entering the boundary layer is reduced. This increases the heat blockage. The combination of effects should drive the temperature down at local hot spots on the matrix, resulting in a reduction of temperature gradients.

The possibility of utilizing a transpiration coolant which undergoes an endothermic reaction has been investigated by Rosner (3), Koh and del Casal (4), and Gorton (5). Rosner points out that because of the relatively short contact time between the matrix and the coolant it may be necessary to have a catalyst present in order to speed the reaction. This would contribute to the realization of as much of the heat absorption potential of the coolant as possible.

Gorton (6) experimentally investigated the use of ammonia as a dissociating transpiration coolant. Ammonia possesses a set of unique properties which make it attractive for use as a transpiration coolant:

- (1) Its dissociation reaction rate is sufficiently fast in the temperature range of interest.
- (2) It has a high heat of formation, 1165 Btu/lb.
- (3) It has a high specific heat.
- (4) It is readily available and relatively inexpensive.
- (5) Commonly used metals (iron, stainless steel, nickel, etc.) are catalysts for the dissociation reaction.
- (6) Only gaseous products are formed.
- (7) The product mixture (containing nitrogen and

hydrogen) have a relatively low molecular weight; 8.5 when the reaction goes to completion.

Combustion of hydrogen (ammonia dissociation product) may occur in the boundary layer. No experimental work to determine the effect of boundary layer combustion on heat transfer in a transpiration cooling system has been done. Meroney (7) used hydrogen as a transpiration coolant, but ignored boundary layer combustion. Rosner (3) discusses boundary layer combustion at some length and suggests that combustion inhibitors might be used to prevent it.

ANALYSIS

Introduction

This report presents a study of the potential of reactive coolants (ammonia) for temperature gradient control. This chapter contains a description of a mathematical model used to simulate a transpiration cooled turbine blade and an analytical comparison of the effectiveness of nitrogen, hydrogen, and ammonia when used as transpiration coolants applied to the model.

Transpiration Cooling System

Figure 1 is a simplified drawing of a transpiration cooling system. The coolant is initially in a reservoir and at a temperature, T_c . As the coolant flows toward the porous matrix, its temperature increases to some temperature T_1 at the inside surface of the matrix ($y=0$). The coolant is then forced through the matrix. The coolant temperature, steadily increases during this period, until it reaches a temperature T_2 , at the outside surface ($y=t$). The coolant then is injected into the free stream, where it eventually reaches the free stream temperature, T_f .

Turbine Blade Model

A turbine blade model was considered ideal for this analysis because of the large variation in the film heating coefficient along the blade. These gave rise to the temperature gradients needed to analytically verify the temperature gradient control feature of ammonia.

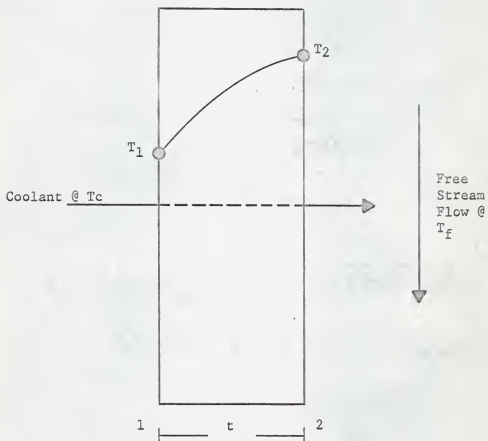


Figure 1. Transpiration cooling system.

The model used to simulate a turbine blade was a streamlined cylinder. Figure 2 is a sketch of the model. The natural coordinate system used is also given. The reference line for the angle theta was the y-axis.

The model was based on a cylinder with a 2 inch radius. The streamlined end was 6 inches long and the wall thickness was .50 inches.

The temperature distribution around the model was assumed to be symmetric about the y-axis line (see Figure 2). Therefore, only half of the model was considered in the analysis.

Analysis

The temperature cooling system was approximated by a set of discrete nodes. A sketch of the half-model with a sample set of nodes is shown in Figure 3. Notice that there were three fundamentally different types of nodes for which heat balances were written; (1) nodes on the coolant reservoir side of the matrix, (2) nodes located in the matrix interior, and (3) nodes on the exterior surface of the matrix.

The difference in length in the x-direction between the outer and inner surfaces was assumed to be negligible. This permitted the use of a rectangular nodal system and simplified the equations considerably.

Before the equations applied to each nodal type are presented, it is necessary to discuss the boundary conditions applied to the problem, to present the method used to estimate the convection coefficients on the model surface, to present the ammonia dissociation reaction rate equation, and to discuss the assumptions made in the problem.

Boundary Conditions

Four boundary conditions were needed to solve the problem. Because

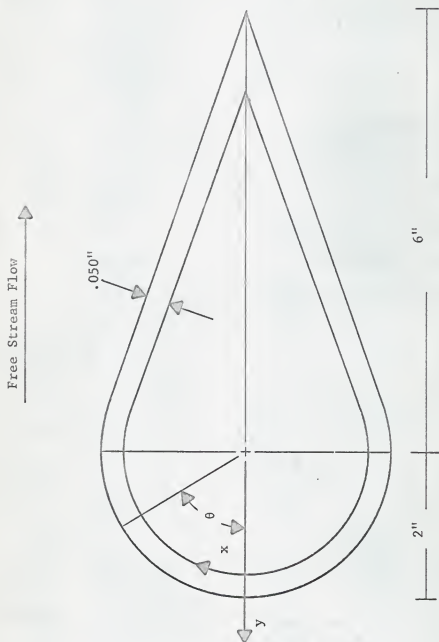
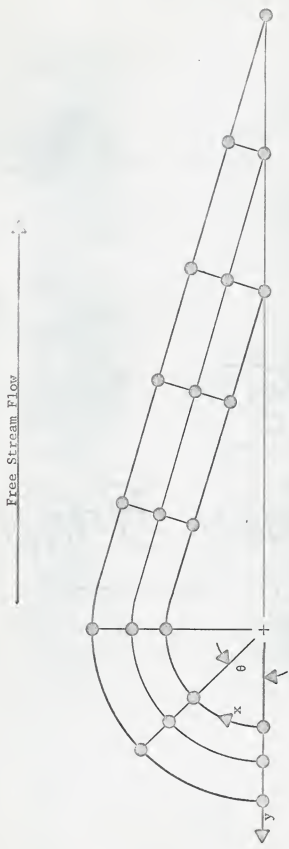


Figure 2. Streamlined cylinder model.



Free Stream Flow

Figure 3. Half-model with sample nodal system. Nodes are based on equal distance at the surface.

of symmetry the two ends were considered to be adiabatic, i.e., no heat transfer across the ends. The boundary condition applied to the outside surface (exposed to free stream) was that the heat conducted was equal to the heat convected. This may be expressed mathematically as:

$$k_s \left. \frac{dT_s}{dy} \right|_2 = h(T_f - T_s) \quad (1)$$

heat conducted heat convected

In order to apply this boundary condition it is necessary to know the values of k_s and h . The boundary condition applied to the coolant reservoir side of the porous matrix was that the heat gain of the coolant, by virtue of its temperature increase from T_c to T_1 , was equal to the heat conducted by the matrix at that surface. Mathematically, this is expressed by:

$$k_s A \left. \frac{dT_s}{dy} \right|_1 = \dot{m}_c'' C_p (T_1 - T_c) \quad (2)$$

heat conducted heat absorbed

To apply this boundary condition, one must know k_s , A , \dot{m}_c'' , and C_p .

Convection Coefficient

The forward portion of the model was a cylindrical surface. The following empirical equation was used to predict the local Nusselt numbers for this part of the model (8).

$$Nu = 1.14(Pr)^{.4} \frac{DU\rho}{\mu}^{.5} \left(1 - \frac{\theta}{90}\right)^{.3} \quad 0^\circ \leq \theta \leq 80^\circ \quad (3)$$

The rear portion of the model was assumed to be a flat plate and the following equation, given by Krieth (9), was applied in this region:

$$\text{Nu}_x = 0.0292 (\text{Re}_x)^{4/5} \cdot (\text{Pr})^{1/3} \quad (4)$$

This equation is used to predict local Nusselt numbers for turbulent flow over a flat plate. Its use here was consistent with the assumption that the cylinder was streamlined. A similar approach was used by Matchett, Colburn, & Ahles (10).

The convection coefficients given by equations (3) and (4) do not account for the effects of mass injection into the boundary layer which occurs during transpiration cooling. In order to correct the coefficients for the mass injection case, Eckert (11) suggests:

$$\frac{\text{St}}{\text{St}_{B=0}} = 1 - C \left(1 - \frac{\beta}{2}\right)^{1/2} \frac{\rho_e}{\rho_w} \frac{M_e}{M_c} \frac{\dot{m}''}{\rho_e U_e \text{St}_{B=0}}^n \quad (5)$$

where C, n, and β are constants. C has a value of 0.73 for laminar boundary layer flow and 0.37 for turbulent boundary layer flow. The value of the exponent, n, on the molecular weight ratio is 1/3 for laminar flow and 2/3 for turbulent flow. The constant β has a value of 0 for flow over a flat plate, 1 for plane stagnation flow, and 1/2 for axially symmetric stagnation flow. The Stanton number for no mass injection, $\text{St}_{B=0}$, is found from equations (3) and (4) in their respective regions of application to the model.

Ammonia Dissociation Reaction Rate Equation

The rate of heat absorption by the dissociation of ammonia may be expressed by $\dot{m} \Delta H \frac{d\alpha}{dy}$. The reaction rate, R_{ch} , is defined as:

$$R_{ch} = \frac{d\alpha}{dy}$$

or

$$\dot{m} \frac{d\alpha}{dy} = PAR_{ch} \quad (6)$$

Introduction of the Arrhenius factor, $e^{-E/RT}$, accounts for the temperature dependence of the reaction rate with:

$$R_{ch} = R_o e^{-E/RT} \quad (7)$$

This assumes a zero order reaction. Substitution of (7) into (6) leads to:

$$\dot{m} \frac{d\alpha}{dy} = PAR_o e^{-E/RT} \quad (8)$$

where T is the temperature of the gas under consideration and R_o is the isothermal reaction rate.

Assumptions

The assumptions made to simplify the problem were:

- (1) The temperature distribution in the model was axially symmetric with respect to the centerline.
- (2) The difference in length in x-direction between outer and inner surfaces was negligible.
- (3) The porous matrix and the coolant were in local thermal equilibrium.
- (4) Operation was at steady state.
- (5) Coolant properties were constant.
- (6) Heat conduction through the coolant fluid was negligible.

- (7) Thermal conductivity of the porous matrix was constant.

The third assumption essentially meant that $T_c = T_s$ everywhere in the porous matrix.

By assuming constant coolant properties a closed form solution is possible for a one-dimensional system with nonreacting coolants (12 and 13). Koh and del Casal (14) have discussed the case of variable coolant properties where the properties are assumed to be power series functions of temperature.

Within the porous matrix, the convection heat transfer completely overwhelms the conduction within the fluid. Therefore, the assumption of negligible heat conduction within the coolant was made.

The conductivity of the matrix was taken to be $k_s (1-P)$.

Discrete Approximation of the System

The finite difference equation used to describe heat flow at nodal points on the interior surface of the model (see Figure 3) was:

$$k_s (1-P) \frac{\Delta y / 2}{\Delta x} (T_{1,n+1} + T_{1,n-1} - 2T_{1,n}) + k_s (1-P) \frac{\Delta x}{\Delta y} (T_{2,n} - T_{1,n}) + \dot{m} C_p (T_c - T_{1,n}) - \Delta x \Delta y P \Delta H R_o e^{-E/RT_{1,n}} = 0 \quad (9)$$

The first and second terms accounted for conduction in the x and y directions, respectively. The third term accounted for the heat absorbed by the coolant as its temperature rose from the reservoir temperature, T_c , to the temperature of the inside surface of the matrix (see Equation 2). The last term represented the heat absorbed by the coolant reaction. For nonreacting coolants the last term was dropped from the equation.

The double subscripts on the temperatures labeled rows and columns of nodal points, respectively. The rows and columns were numbered in ascending order from front to rear and from inside surface to outside surface.

The equation used to describe heat flow at nodal points inside the matrix was:

$$k_s (1-P) \frac{\Delta y}{\Delta x} (T_{m,n+1} + T_{m,n-1} - 2T_{m,n}) + k_s (1-P) \frac{\Delta x}{\Delta y} (T_{m+1,n} + T_{m-1,n} - 2T_{m,n}) + \dot{m} C_p (T_{m-1,n} - T_{m,n}) - \Delta x \Delta y P \Delta H_{R_0} e^{-E/RT_{m,n}} = 0 \quad (10)$$

The explanation of the first, second, and last terms is the same for equation (10) as for equation (9). The third term represented the heat absorption of the coolant by virtue of its temperature increase in moving from the corresponding node in the preceding row to the node under consideration.

Heat flow for nodal points on the exterior surface of the cylinder was described by:

$$k_s (1-P) \frac{\Delta y/2}{\Delta x} (T_{m,n+1} + T_{m,n-1} - 2T_{m,n}) + k_s (1-P) \frac{\Delta x}{\Delta y} (T_{m-1,n} - T_{m,n}) + \dot{m} C_p (T_{m-1,n} - T_{m,n}) - \Delta x \Delta y P \Delta H_{R_0} e^{-E/RT_{m,n}} + h_f \Delta x (T_f - T_{m,n}) - 0 \quad (11)$$

where the subscript m was the number of the label for the row of nodes at the outside surface. The explanation of the first four terms was the same as for equation (10). The fifth term described the convection heat transfer to the matrix from the mainstream (see Equation 1).

The general method of solution involved choosing a grid of nodal points, writing the equation applicable to each node, and solving the resulting system of simultaneous equations. The simultaneous equations in the analysis were solved on a digital computer using the method of iteration by total steps as described by Crandall (15).

Appendix A contains a listing of the computer program. Comment cards at the beginning of the program explain the input parameters needed.

Results and Discussion

The freestream gas considered was air with the following input parameter values:

1. $Re_D = 100,000$ (corresponding to a velocity of approximately 830 ft/sec for air).
2. $T_f = 2500^\circ F$
3. $\mu_f = 3.69 (10^{-5}) \text{ lb}_m/\text{ft-sec}$
4. $p = 1 \text{ atm.}$
5. $\rho = .0133 \text{ lb}_m/\text{ft}^3$
6. $Pr_f = .763$

The reservoir temperature and pressure of all the coolants were taken as:

1. $T_c = 400^\circ F$
2. $p = 1 \text{ atm.}$

The values of the coolant properties required by the program (specific heat, Prandtl number, and thermal conductivity) were evaluated at these conditions for each coolant.

The porous matrix material was stainless steel. The value of thermal conductivity input for the matrix was $13.5 \text{ Btu/hr-ft-}^\circ F$.

The E/R value in the exponential power was input as $9500^{\circ}\text{R}^{-1}$ (6).

The blowing rate was an input parameter. Its value was chosen to be within the range of blowing rates used in previous transpiration cooling experiments.

The first case studied was transpiration cooling with nitrogen. The blowing rate parameter chosen was .003. The results are plotted in Figures 4 and 5.

Hydrogen was considered as a transpiration coolant in the second case. The results are plotted in Figures 4 and 5, along with the results of the first case. Two blowing rates were considered for the hydrogen case; $F = .0003$ and $F = .0008$. At a blowing rate of .0003, hydrogen maintained approximately the same outer surface temperatures as nitrogen at $F = .003$. The temperature gradient in the x-direction was somewhat reduced by hydrogen when compared with nitrogen, however the gradient in the y-direction was significantly increased.

Ammonia, with its accompanying dissociation reaction, was studied in the third case. The results are shown in Figures 6 and 7. Three blowing rates were considered for ammonia; $F = .0003$, .0008, and .003. Comparing Figures 4 and 6 reveals that ammonia, with a blowing rate of .0008, maintained approximately the same surface temperatures as hydrogen at a blowing rate of .0003 and nitrogen at .003. In these comparison runs the temperature gradients in both the x and y-directions were less for the ammonia case than for either of the other two cases (Figures 4,5,6, and 7). In Figures 6 and 7 it may be seen that as the ammonia blowing rate was reduced, the temperature gradients in both the x and y-directions were reduced, even though the actual matrix temperatures increased. This was attributed

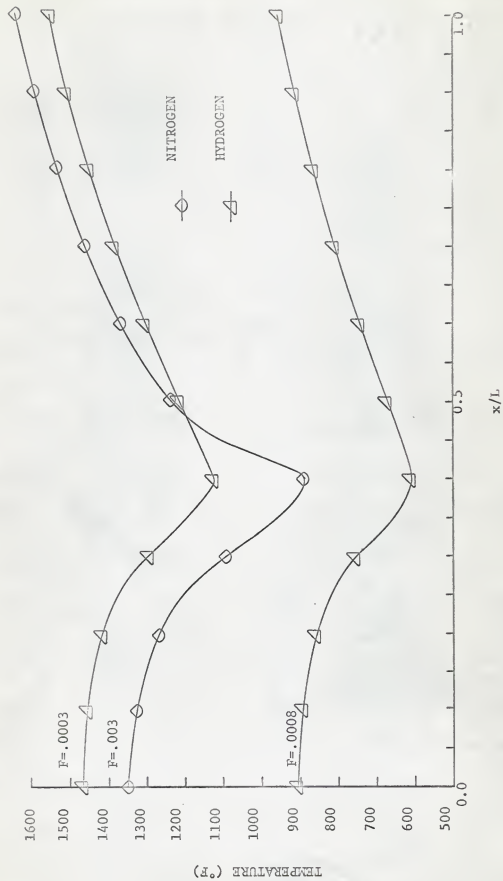


Figure 4. Temperature versus x/L for transpiration cooling with hydrogen and nitrogen (temperatures for outside surface).

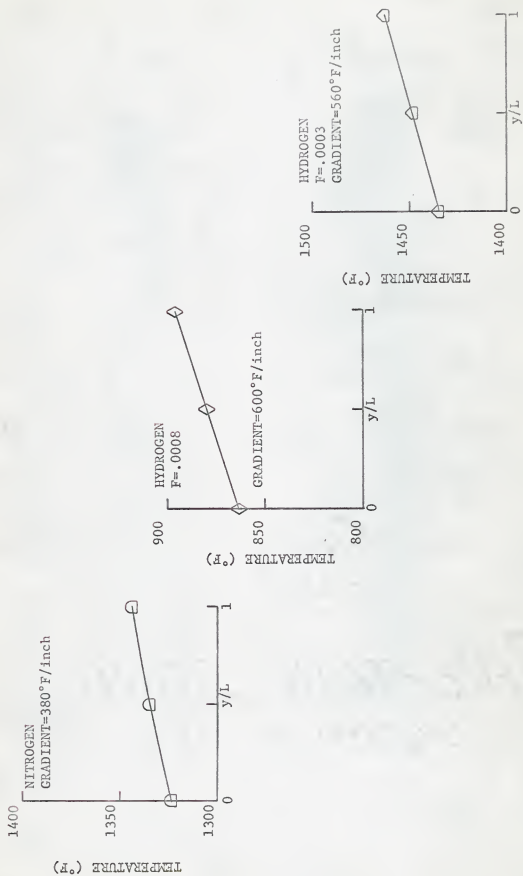


Figure 5. Temperature versus y/L at forward stagnation point for nitrogen and hydrogen.



Figure 6. Temperature versus x/L at forward stagnation point for ammonia.

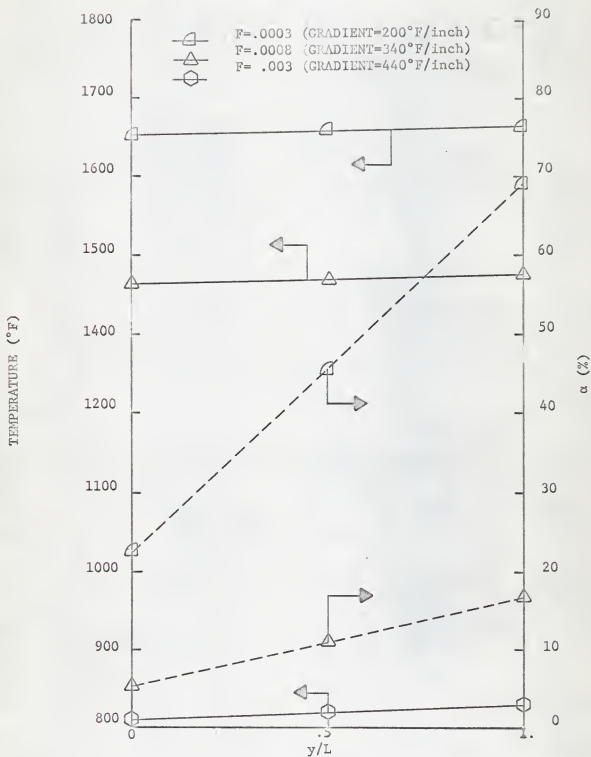


Figure 7. Temperature and fraction of coolant dissociated versus y/L for ammonia (dotted lines are for dissociation). The percent of dissociation for $F=.003$ was too low to plot on this coordinate system.

to the greater amount of dissociation which occurred at lower ammonia flow rates (Figure 7).

The conclusions drawn from the analysis were:

- (1) Hydrogen was the most effective at reducing matrix temperatures, on a blowing rate basis, of the three transpiration coolants studied. The use of hydrogen as a coolant did result in large temperature gradients, particularly in the y-direction.
- (2) Temperature gradients within the porous matrix could be significantly reduced by using ammonia as a transpiration coolant.

EXPERIMENT

Introduction

To substantiate the above conclusions, an experimental program was begun. The purposes of the experiment were to compare ammonia, hydrogen, and nitrogen as transpiration coolants in a high temperature combustion gas stream and to verify the predicted ammonia reaction effect of reducing temperature gradients.

To accomplish these objectives a cylinder was chosen as a porous sample shape. The cylinder was chosen for two reasons. First, it was an easy geometry to fabricate and second, it provided a large variation of convection coefficients on the surface. This variation of convection coefficients gave rise to the matrix temperature gradients needed to verify the ammonia reaction effect.

Apparatus

The apparatus used in the experiment consisted of five parts; (1) a propane burner and hot gas mixing tube, (2) a test section, (3) an exhaust fan and duct, (4) a sample with its associated mechanical fixtures, and (5) instrumentation. A schematic of the system is shown in Figure 8.

The burner was a Wondaire Model PG-260B. This unit was capable of producing 280,000 Btu's per hour. Hot gases from the burner were released inside a 6 1/2 inch diameter ceramic tube, 6 feet in length. The ceramic tube served two purposes; mixing of the hot gases and reducing heat losses

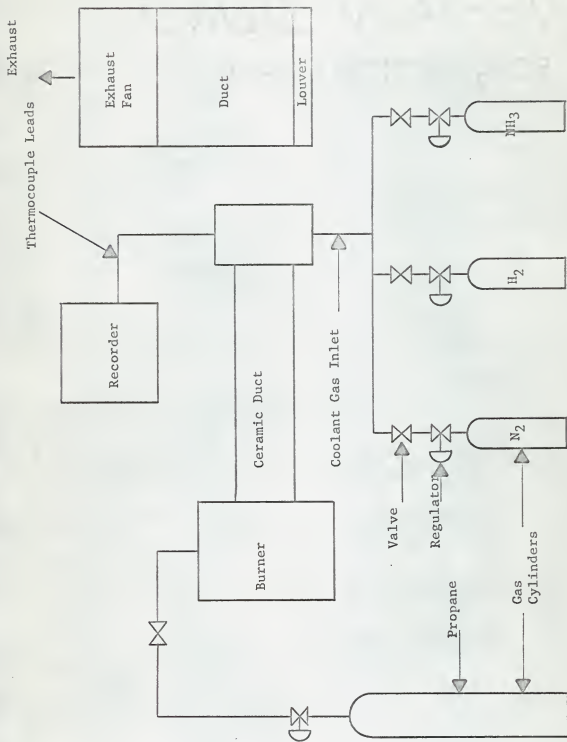


Figure 8. Schematic diagram of experimental apparatus.

from the system to a minimum.

At the end of the ceramic tube, the hot gases entered a 14 inch long section of 6 inch diameter iron pipe. The end of this pipe had two short pieces of channel iron welded into its walls (Figure 9). The large flat faces of the channel irons were opposite and parallel, changing the duct shape from circular to nearly rectangular. This was the test section. Each flat face had a $1 \frac{9}{16}$ inch diameter hole in it. The holes were aligned to allow the sample cylinder to be inserted through them into the test section.

From the test section, the hot gases next entered the exhaust system. A louver on the open end of the duct permitted control of the amount of room air entering it. The hot gases were pulled into the duct through a port in its side. Room air and exhaust gases were mixed in the duct and then forced through a window by the axial flow exhaust fan.

Figure 10 is a drawing of the porous sample with its associated hardware. Two different sizes of samples were used. The first was $1 \frac{1}{2}$ inches in outside diameter with $\frac{1}{4}$ inch thick walls. The second had a 1 inch outside diameter with $\frac{1}{16}$ inch thick walls. Both samples were 4 inches in length and were constructed of sintered stainless steel. Also, both samples had a 40 micron filtration rating. Although the samples were different, the mechanical fixtures used to seal the ends and inject the coolant were basically the same, having only minor dimensional differences. The coolant was injected into the cylinder through a $\frac{1}{4}$ inch stainless steel tube. The tube had a series of small holes in its surface to allow dispersion of the coolant inside the cylinder. The end of the tube was sealed by brazing a 3 inch long, $\frac{1}{4}$ inch threaded rod in it. The end caps for the cylinder had circular groves machined in them. Asbestos

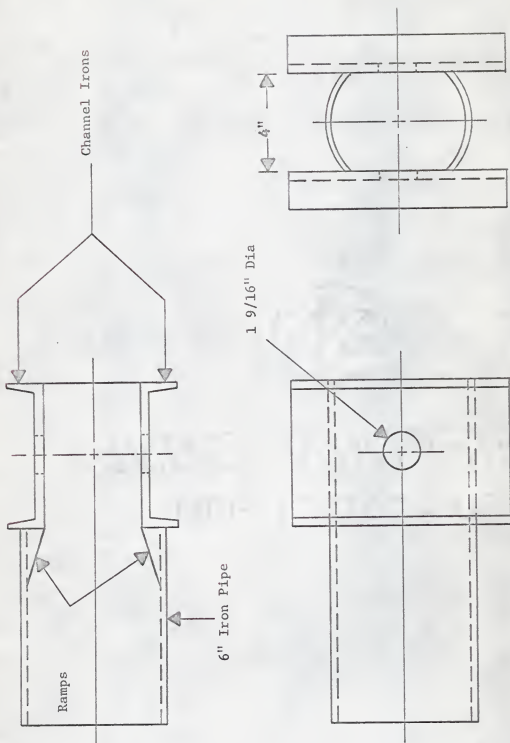


Figure 9. Iron pipe and test section.

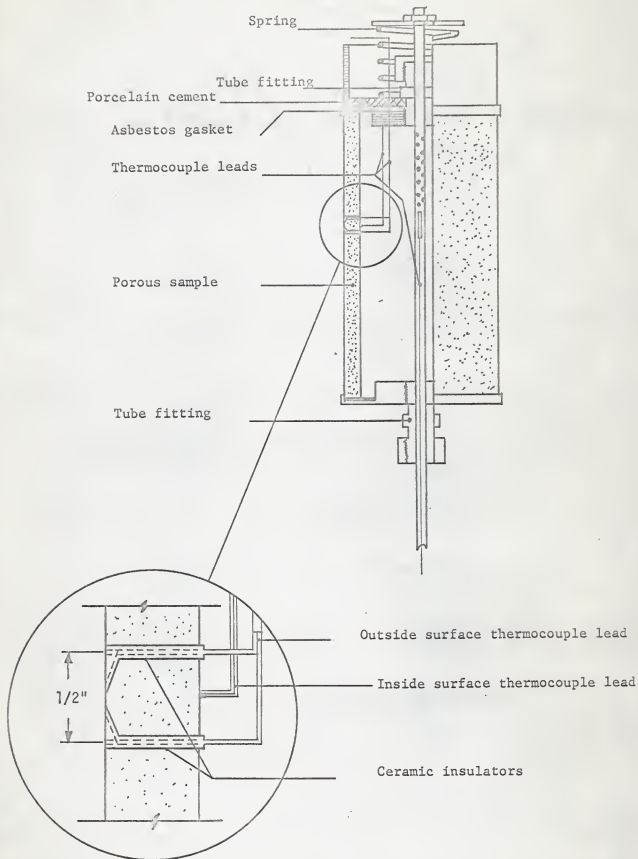


Figure 10. Porous sample and associated hardware.

gaskets were set in the groves. The cylinder ends were then inserted in the groves. The coolant tube was inserted in the cylinder through Swagelok fittings in the end caps. The fitting on the coolant entrance side was tightened making the cap on that end immobile with respect to the coolant tube. In order to allow for thermal expansion of the sample, it was necessary that the other end cap (which had the 1/4 inch threaded rod protruding from its fitting) be free to move parallel to the axis of the cylinder. This was accomplished by compressing a spring against the end cap. The spring exerted a compressive force on the cylinder-gasket-end cap system, thereby helping to seal the ends. The fitting at the spring end was sealed by wrapping its parts with Teflon tape and partially tightening the fitting.

The most important part of the instrumentation was the thermocouple mounting in the porous cylinders (see Figure 10). Chrome-alumel thermocouples with fiberglass insulation were used. Thermocouples on the 1 1/2 inch diameter cylinder were mounted on both the outside surface and the inside surface. The wall of the 1 inch cylinder was assumed to be thin enough that the temperature gradient across it was negligible, therefore thermocouples were mounted only on the inside of this sample. In order to measure the outside surface temperature of the 1 1/2 inch sample as accurately as possible it was necessary to minimize disturbance of the coolant flow in the vicinity of the thermocouple. This was accomplished by separating the two thermocouple wires and stringing them through separate, ceramic insulated, holes. These holes were located at the middle of the cylinder about 1/2 inch apart on a line parallel to the longitudinal axis of the cylinder. The ends of the wires were bent over towards each other and welded into tapered slots, leaving a gap between their ends of about

1/8 inch. The holes were sealed with Saucereisen porcelain cement. Thermocouples mounted on the insides of the samples were merely welded in place. Figure 11 shows the thermocouple installation positions along with the numbering system used to identify them. The thermocouple leads extended through holes in the end cap at the spring end of the cylinder. The thermocouple outputs were recorded on a Speedomax, type G, twenty point recorder.

A thermocouple was installed in the coolant injection tube to measure the coolant reservoir temperature, (see Figure 10). The output was measured with a manual balance potentiometer instead of using the recorder because of range mismatch between the recorder input and the reservoir thermocouple output.

A system of piping and valves allowed selection of the desired coolant (see Figure 8). The coolant flow rate was measured with a rotameter. The temperature and pressure of the coolant was measured as it left the rotameter by means of a mercury thermometer and Bourdon-type pressure gauge, respectively.

The fuel flow rate to the burner was measured with a rotameter.

The fuel and coolant rotameters were calibrated by means of a positive displacement American gas meter.

Procedure

Startup of the system merely involved opening the propane supply valve and activating the burner relay and ignition circuits. The burner then started automatically and when the flame was established the exhaust fan was started. The system took approximately one hour to reach steady state due to the long warmup period for the ceramic duct.

Velocity and temperature profiles were measured in the test section

in order to find the free stream temperature and estimate the product ρU . A thermocouple probe was used for the temperature traverse and a pitot tube was used to measure the pressure profile from which the velocity profile was calculated. The test section centerline was used as a reference with measurements being taken there and at 1/2 inch intervals from the centerline to both walls. The traverses were done parallel to the axis of the sample installation holes.

Tests were run on the 1 1/2 inch cylinder first. The cylinder was inserted in the test section with thermocouple #1 at the front stagnation point, (see Figure 11). This caused thermocouple #2 to be located at a point 90° clockwise from the stagnation point. After the temperature readings reached steady state, the cylinder was rotated clockwise 15°. After steady state temperatures were reached the cylinder was rotated another 15°. This procedure was repeated for two more 30° rotations, for a total of 90°, ending with thermocouple #2 at the back stagnation point. It took approximately 10 minutes for the temperatures to reach steady state at each station. For the next data set either the coolant type, the coolant flow rate, or the burner fuel flow rate was changed and the cylinder rotation procedure reversed. The coolants were run in the following order; (1) nitrogen, (2) hydrogen, and (3) ammonia.

The test procedure for the 1 inch diameter cylinder differed in that the temperatures from 0° to 180° were measured at 45° increments simultaneously by its five thermocouples (see Figure 11). Ammonia was the only coolant used with this sample.

Results

Three data runs were performed with 1 1/2 inch cylinder. The first run

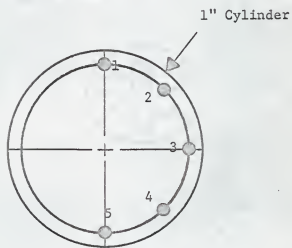
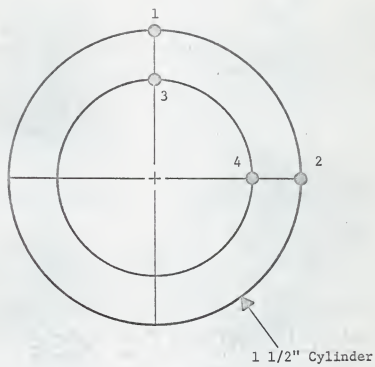


Figure 11. Thermocouple locations. The thermocouples were mounted at the center of the cylinder.

was made using nitrogen as a coolant. The blowing rate for this run was .00583. The burner fuel flow rate was .88 cubic feet per minute, giving a centerline temperature in the test section of 1170°F. Ammonia was used as a coolant in the second run. The blowing rate was .00478 and the burner fuel flow rate was the same as in the first run. The third run was also performed with ammonia. The burner fuel flow rate was 1.08 cubic feet per minute, giving a centerline temperature of 1380°F. The ammonia flow rate was the same in the third run as it was in the second, however, the extra fuel mass in the free stream resulted in a slight decrease in the blowing rate to .00482. The results of these three runs are plotted in Figures 12 and 13. Comparison of the plots in Figure 12 for the first two runs indicates that ammonia was a more effective coolant than nitrogen (identical free stream conditions). Use of ammonia resulted in lower matrix temperatures than nitrogen, even though the ammonia blowing rate was less than that of nitrogen. The matrix temperatures were increased considerably in the third run over the temperatures obtained in the second run. A temperature rise was expected because the free stream temperature was higher, however, the matrix temperature increase in the vicinity of the forward stagnation point was greater than the increase in free stream temperature. There was no apparent reduction in temperature gradients along the surface or through the wall of the sample (see Figure 13).

Combustion in the boundary layer was observed in the forward stagnation region during the second and third runs.

Near the end of the third run, a slight bulge appeared near the front of the cylinder. Another run with ammonia was attempted, but before any data could be taken the bulge had become a rupture and it was obvious the sample

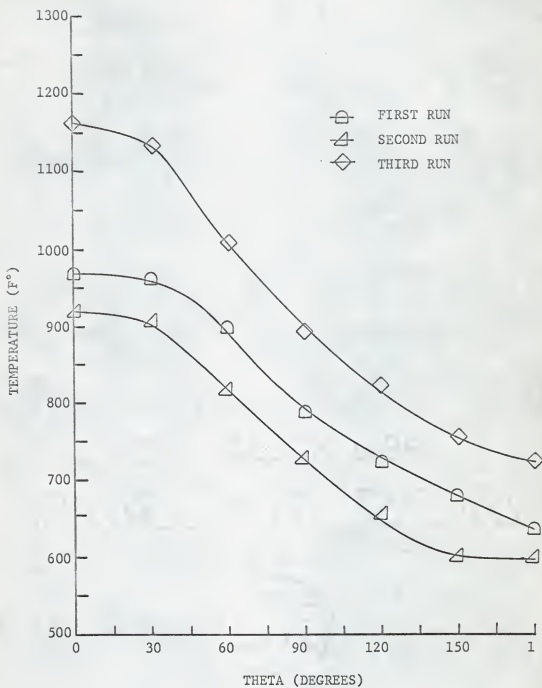


Figure 12. Exterior surface temperature versus theta for 1 1/2 inch cylinder.

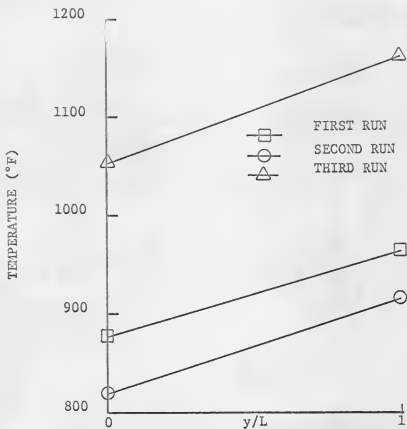


Figure 13. Temperature versus y/L at forward stagnation point for 1 1/2 inch cylinder.

was ruined.

A hydrogen run was attempted between the first and second runs. This run was abandoned because the matrix temperature increased very rapidly and showed no signs of reaching equilibrium before it attained a temperature level at which failure seemed imminent. Combustion in the boundary layer was observed during the time the hydrogen was being injected into the sample

Ammonia was the only coolant used with the 1 inch cylinder. The burner fuel flow rate was .88 cubic feet per minute for all three data runs performed with this sample. The only parameter that was varied for these runs was the blowing rate. Blowing rates of .00776, .00533, and .00364 were used for the first, second, and third runs on the 1 inch cylinder, respectively. The results of these runs are presented in Figure 14. Lower coolant blowing rates resulted in higher matrix temperatures, as expected. No reduction of temperature gradients between the forward and back stagnation points occurred as the blowing rate was lowered (more ammonia dissociation occurred at lower blowing rates). The gradient actually increased 60°F in going from the highest blowing rate to lowest blowing rate. This sample failed in a manner similar to the first sample.

Appendix B contains a summary of the data.

Conclusions

Extensive examination of the rather meager data and the samples was undertaken to determine why the samples failed and why the temperature gradients were not reduced as predicted.

There were several similarities between the failures of the two samples. Both failed in the region of the forward stagnation point. The

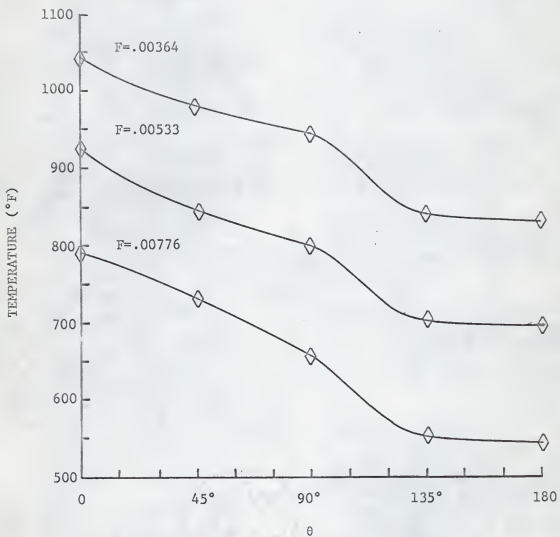


Figure 14. Temperature versus theta for 1 inch cylinder.

material in the areas of the failure looked the same for both. Swelling and extensive cracking had occurred and the material in these areas had a burned appearance. Both failures occurred during ammonia runs.

There were two possible reasons why the samples failed and the temperatures gradients were not reduced. The first possibility was extreme convection heating in the forward stagnation region caused by boundary layer combustion. This extreme local heating at the forward region could have caused the sample failures. It also could have given rise to the large temperature gradients obtained due to severe uneven heating of the sample. Boundary layer combustion could also explain why the temperature at the forward stagnation point on the 1 1/2 inch cylinder increased more than the increase in free stream temperature between the second and third runs. The higher temperature of the third run considerably increased the amount of dissociation calculated (see Appendix B) to have occurred. This in turn released more hydrogen to burn in the boundary layer thereby increasing the convection heating received by the sample, and causing the large temperature increase, leading to the failure of the sample. The failure of the 1 inch cylinder could be explained in much the same manner. Reduction in the blowing rate caused an increase in sample temperature resulting in more dissociation (calculated; see Appendix B). This increased the amount of hydrogen in the boundary layer available for combustion, etc.

The second possible cause of sample failure was non-uniform coolant flow distribution. Since the free stream pressure was greatest at the forward stagnation point, more coolant would be forced to flow out the backside of the cylinder. This could explain the extreme heating at the front of the cylinder, which was left relatively unprotected due to the reduced coolant

flow through that region, and the ultimate thermal failure. This type of uneven coolant flow would also have produced large temperature gradients around the cylinder.

It was felt that the most probable cause of the difficulties was boundary layer combustion because of two facts. First, the free stream velocity was relatively slow (15 feet per second), causing very small pressure variation around the cylinder. Secondly, the failures occurred during the ammonia runs which were the only successful data runs where combustion could occur. Boundary layer combustion was observed during both ammonia runs with the 1 1/2 inch cylinder. Combustion in the boundary layer was also observed during the one run that was attempted with hydrogen. Combustion in the boundary layer was not seen to occur on the second sample. However, the front of the sample could not be observed due to the construction of the test section, therefore, combustion could have occurred at the very front without being seen. The calculated amount of dissociation at the front stagnation point was very low for the second sample (see Appendix B), so the small amount of hydrogen produced could have burned at the front of the cylinder. By the time the boundary layer carried the mass injection products around to an observable part of the cylinder surface, the hydrogen produced could have already been burned. It was proven to this investigator's satisfaction that combustion caused the difficulties (by comparing the experimental results with results obtained from an analysis using the program described in the preceding chapter of this paper).

Interpretation of Experimental Results in Light of Analytical Results

Four runs were made with the program using a model based on the 1 1/2 inch cylinder. The free stream conditions, blowing rates, and coolant

reservoir temperatures were input to the program using conditions corresponding to the experimental data runs. The input to the first three computer runs was meant to duplicate the conditions of the three experimental data runs made on the 1 1/2 inch cylinder. The fourth run duplicated the conditions of the second experimental data run, except that no dissociation was allowed in the computation. The results are plotted in Figure 15. The mathematical model used was a streamlined cylinder, therefore, only the results obtained for the 0°, 30°, and 60° points in the experimental data can be validly compared to the corresponding results obtained from the analysis. With this in mind, comparison of the experimental and analytical results for the nitrogen coolant at these points reveals that the analysis predicted matrix temperatures within 50°F of the measured results. This indicates that the coolant flow was fairly well distributed (uniform distribution was assumed in the program). Comparison of the corresponding ammonia runs shows large differences between the analytically and the experimentally obtained results. The fact that the experimentally obtained temperatures were so much greater than the analytical predictions, in view of the fact that the coolant flow was uniformly distributed, indicates that combustion in the boundary layer did in fact cause the poor performance of ammonia as a transpiration coolant. Combustion also was the probable reason why no data was obtained for hydrogen.

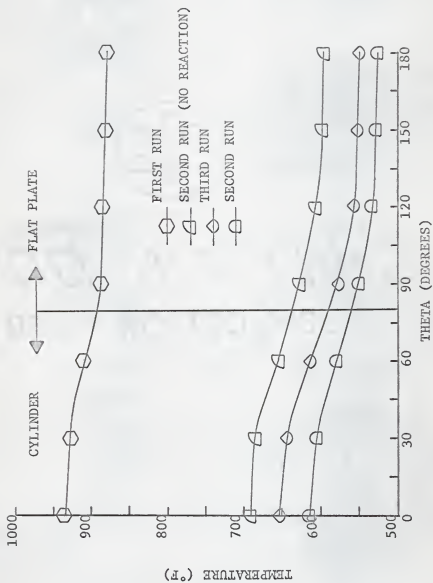


Figure 15. Temperature versus theta found analytically for 1 1/2 inch cylinder.

SUMMARY

On paper, ammonia appears to be an almost ideal transpiration coolant for immersed bodies experiencing extreme convective heating due to high free stream temperatures. However, in practice, this does not seem to be true due to the high heating rates imposed by boundary layer combustion of hydrogen (ammonia dissociation product). Much more work needs to be done in this field. Some suggestions for future work include:

1. Experimentation with combustion inhibitors.
2. Investigation of effects of boundary layer combustion.
3. Investigation of pressure gradient effects on transpiration coolant flow distribution from immersed bodies.

REFERENCES

1. Leadon, B.M. "The Status of Heat Transfer Control by Mass Transfer for Permanent Surface Structure." Aerodynamically Heated Surfaces, pp. 171-196. Englewood Cliffs: Prentice-Hall, 1962.
2. Kelly, J.B., and M.R. L'Ecuyer. "Transpiration Cooling--Its Theory and Application." TM-65-5, Purdue University, Jet Propulsion Center, Research Report, Lafayette, Indiana, June, 1966.
3. Rosner, D.E. "Transpiration Cooling with Chemical Reactions," TP-79, Aero Chem Research Laboratories, Research Report, Princeton, New Jersey, January, 1964.
4. Koh, J.C.Y., and E.D. del Casal. "Heat and Mass Transfer with Chemical Reactions for Fluid Flow through a Porous Matrix in Re-entry Thermal Protection." AIAA Paper No. 66-423, June, 1966.
5. Gorton, R.L. "An Analysis of the Effect of Use of Reactive Coolants in Porous Body Cooling." ASME Paper No. 68-H-124, 1968.
6. Gorton, R.L. "An Experimental Study of Ammonia as a Reactive Transpiration Coolant." ASME Paper No. 68-H-35, 1968.
7. Meroney, R.N. "Experimental Investigation of the Effects of Transpiration Cooling on a Partially Dissociated Turbulent Boundary Layer." AS-63-6, University of California, Institute of Engineering Research, Research Report, Berkeley, California, November, 1962.
8. Knudsen, J.F., and D.L. Katz. Fluid Dynamics and Heat Transfer. New York: McGraw-Hill Book Company, 1958.
9. Krieth, Frank. Principles of Heat Transfer. Second edition. Scranton: International Textbook Co., 1966.
10. Matchett, J.D., J.N. Colburn, and A.F. Ahles. "A Comparison of Calculated and Measured Temperature Distributions in Forced-Convection Air-Cooled Gas Turbine Airfoils." ASME Paper No. 67-WA/GT-4, 1967.
11. Eckert, E.R.G. "Survey of Boundary Layer Heat Transfer at High Velocities and High Temperatures." 59-624, University of Minnesota, WADC Technical Report, Minneapolis, Minnesota, April, 1960.

12. Schneider, P.J. Conduction Heat Transfer. Reading: Addison-Wesley Publishing Co., 1955.
13. Green, L., Jr. "Gas Cooling of a Porous Heat Source." Journal of Applied Mechanics, Trans ASME. 74, Series E: 173-178, 1952.
14. Koh, J.C.Y., and E.D. del Casal. "Heat and Mass Flow Through Porous Matrices for Transpiration Cooling." Heat Transfer and Fluid Mechanics Inst., pp. 261-281. Stanford: Stanford University Press, 1965.
15. Crandall, S.H. Engineering Analysis. New York: McGraw-Hill Book Co., 1956.

NOMENCLATURE

English Symbols

A = area

C_p = specific heat

D = diameter

E = activation energy

F = blowing rate ($\rho V/\rho U$)

h = convection heat transfer coefficient

ΔH = heat of dissociation at T_f

k = thermal conductivity

\dot{m} = mass flow rate

\dot{m}'' = mass flow rate per unit area

Nu = Nusselt number ($h \cdot \text{characteristic length}/k$)

P = porosity

p = pressure

Pr = Prandtl number ($\mu C_p/k$)

R = gas constant

R_{ch} = temperature dependent reaction rate

Re = Reynolds number ($\rho V D/\mu$)

R_o = isothermal reaction rate

St = Stanton number ($h/\rho C_p V$)

T = temperature

t = wall thickness
 U = velocity of free stream
 V = velocity
 x = length coordinate
 y = thickness coordinate

Greek Symbols

α = fraction of coolant dissociated
 ρ = density
 μ = dynamic viscosity
 θ = angle from the leading edge

Subscripts

1 = of the surface on coolant reservoir side of porous material
 2 = of the surface on free stream side of porous material
 $B=0$ = at zero blowing rate
 C = of the coolant reservoir
 D = based on diameter
 e = at the outer edge of the boundary layer
 f = of the free stream
 m = integer for subscripted variables
 n = integer for subscripted variables
 s = of the porous material
 x = based on distance measured from the leading edge
 $*$ = at the Rubesin-Eckert reference state

APPENDICES

APPENDIX A

This appendix contains a printout of the computer program used in the analytical section.

```

C      N-NUMBER OF NODAL POINTS
C      M-NUMBER OF POINTS IN Y-DIRECTION
C      NOTE-N/M MUST BE AN INTEGER
C      TF-TEMPERATURE OF FREE STREAM
C      TC-TEMPERATURE OF COOLANT INSIDE CYLINDER
C      RED-REYNOLDS NUMBER BASED DIAMETER OF CYLINDER
C      D-DIAMETER OF CYLINDER IN INCHES
C      NOTE-THICKNESS OF WALL MAY BE CHANGED BY CHANGING
C      NUMERATOR OF DY CARD IN MAIN PROG
C      P-POROSITY OF MATRIX
C      DVF-DYNAMIC VISCOSITY OF FREE STREAM
C      CP-SPECIFIC HEAT OF COOLANT
C      CKS-CONDUCTIVITY OF MATRIX (SOLID)
C      CKF-CONDUCTIVITY OF FREE STREAM GAS
C      PRF-PRANDTL NUMBER OF FREE STREAM
C      REDC-RFYNOLDS NUMBER OF COOLANT FOR ORDINARY DUCT
C      CONVECTION COOLING
C      DL-NUMBER OF INCREMENTS IN X-DIRECTION (AROUND CYL.)
C      TW-WALL TEMPERATURE DESIRED IN ORDINARY DUCT
C      CONVECTION
C      CKC-CONDUCTIVITY OF COOLANT AT TC
C      PRC-COOLANT PRANDTL NUMBER
C      IREA-INPUT PARAMETER
C           =1-FOR REACTING COOLANT
C      DH-HEAT OF FORMATION OF COOLANT
C      NOTE-BLOWING RATE MAY BE CHANGED BY CHANGING
C      F CARD IN MAIN PROG
C      NOTE- WEIGHT RATIO CHANGE BY CHANGING WR CARD
C      INPUT TO SUBROUTINE STR
C           X(N)-TEMPERATURE GUESS FOR EACH NODE
C      DIMENSION A(100,101),HF(100)
C      COMMON N,DX,DY,P,DH,RO,RVC,NM,NM1,IREA
1  FORMAT(18HOSPARATION OCCURS/)
2  FORMAT(1H0,8X,1HX,15X,2HHF,12X,1HI/)
3  FORMAT(1H ,2F16.8,2X,I3)
4  FORMAT(214,2X,3F8.0,F4.2)
5  FORMAT(6F10.8)
6  FORMAT(3H K=,I3,5X,2HL=,I3)
7  FORMAT(3F10.2,2F10.8)
8  FORMAT(1I,2X,F10.8)
9  FORMAT(3H N=,3X,I3,14X,2HM=,2X,I3,15X,3HTF=,
10 11X,E16.8,2X,3HTC=,1X,E16.8,2X,4HRED=,E16.8)
11 12  FORMAT(3H D=,2X,E16.8,2X,2HP=,2X,E16.8,2X,
13 14H DVF=,E16.8,2X,3HCP=,1X,E16.8,2X,4HCKS=,E16.8)
14 13  FORMAT(5H CKF=,E16.8,2X,4HPRF=,E16.8,2X,5HREDC=,
15 14E15.8,2X,3HDL=,1X,E16.8,2X,3HTW=,1X,E16.8)
16 14  FORMAT(5H CKC=,E16.8,2X,4HPRC=,E16.8,2X,5HIREA=,
17 15I2,15X,3HDH=,1X,E16.8,2X,3HWR=,1X,E16.8)
18 15  FORMAT(4H DR=,1X,E16.8,2X,2HF=,2X,E16.8,2X,3HDX=,
19 1611X,E16.8,2X,3HDY=,1X,E16.8,2X,4HRVC=,E16.8)

```

```

16 FORMAT(4H HC=,1X,E16.8/)
  READ(1,6) N,M,TF,TC,RED,D
  READ(1,7) P,DVF,CP,CKS,CKF,PRF
  READ(1,9) REDC,DL,TW,CKC,PRC
  READ(1,10) IREA,DH
  R0=132.*1778.
  DL=1.0/DL
  N1=N+1
  WR=1.703
  DR=1.0
  PRR=1.0
  PRP=1./3.
  PRP2=2./3.
  LL=1
  PI=3.14159265
  F=.00487
  NM=N/M
  NM1=NM+1
  L=1
  K=1
  D=D/12.
  XX=NM-1
  SEPX=(2./9.)*PI*D
  YY=M-1
  DX=(PI*D/2.)/XX
  X=0.
  DY=.250/(12.*YY)
  RVC=F*RED*(DVF/D)
  C1=DY/DX
  C2=DX/DY
  C3=DX/(CKS*(1.-P))
  C4=(RVC*3600.*DX*CP)/(CKS*(1.-P))
  C5=C1/2.
  C6=CKS*(1.-P)
  C7=C1*C6
  C8=C2*C6
  S=(PRC**PRP)*(REDC**P)*((TC/TW)**.15)
  R=.020*(1.+(DL**.7))*(CKC/D)
  HC=S*R
  WRITE(3,11) N,M,TF,TC,RED
  WRITE(3,12) D,P,DVF,CP,CKS
  WRITE(3,13) CKF,PRF,REDC,DL,TW
  WRITE(3,14) CKC,PRC,IREA,DH,WR
  WRITE(3,15) DR,F,DX,DY,RVC
  WRITE(3,16) HC
  DO 101 I=1,N
  DO 102 J=1,N1
102 A(I,J)=0.
101 CONTINUE
  MI=N1-NM

```

```

DO 104 KK=MI,N
  IF(X.GE.SEPX) GO TO 205
  HF(KK)=1.01*(RED**.5)*(1.-(((4.*X)/(D*PI))**.3))
  HF(KK)=(CKF/D)*((HF(KK)*PRR)-.73*(.75**.5)
1*DR*(WR**PRP)*RVC*PRF*(D/DVF))
  GO TO 206
205 HF(KK)=.0292*((RED*(X/D))**.8)*(PRF**PRP)
  HF(KK)=(CKF/D)*((HF(KK)*PRR)-.37*(.75**.5)
1*DR*(WR**PRP2)*RVC*PRF*(D/DVF))
  IF(LL.EQ.1) WRITE(3,1)
  LL=LL+1
206 IF(KK.EQ.MI) WRITE(3,2)
  WRITE(3,3) X, HF(KK), KK
  X=X+CX
104 CONTINUE
  DO 103 I=1,N
  WRITE(3,8) K,L
  J=I
  J1=J+1
  J2=J-1
  J3=J-NM
  J4=J+NM
  IF(L.EQ.1) GO TO 201
  IF(L.EQ.N) GO TO 200
  A(I,J)=-2.*(C7+C8)-(RVC*CP*3600.*DX)
  IF(K.EQ.1) GO TO 202
  A(I,J2)=C7
  IF(K.EQ.NM) GO TO 211
  A(I,J1)=C7
  GO TO 203
211 A(I,J2)=2.*C7
  GO TO 203
202 A(I,J1)=2.*C7
203 A(I,J3)=C8+(RVC*CP*3600.*DX)
  A(I,J4)=C8
  K=K+1
  IF(K.EQ.NM1) GO TO 204
  GO TO 103
204 K=1
  L=L+1
  GO TO 103
200 A(I,J)=- (C1+C2+(C3*HF(I))+C4)
  A(I,J3)=C4+C2
  A(I,N1)=- (HF(I)*DX*TF)/C6
  IF(K.EQ.1) GO TO 207
  A(I,J2)=C5
  IF(K.EQ.NM) GO TO 208
  A(I,J1)=C5
  GO TO 209
208 A(I,J2)=2.*C5

```

```
GO TO 209
207 A(I,J1)=2.*C5
209 K=K+1
IF(K.EQ.NM1) GO TO 210
GO TO 103
210 K=1
L=L+1
GO TO 103
201 IF(F.LT..000001) GO TO 300
A(I,J)=- (2.*C6*C5)-C8-(RVC*CP*3600.*DX)
A(I,N1)=- (RVC*CP*TC*3600.*DX)
A(I,J4)=C8
IF(K.EQ.1) GO TO 212
A(I,J2)=C6*C5
IF(K.EQ.NM) GO TO 213
A(I,J1)=C6*C5
GO TO 214
212 A(I,J1)=2.*C6*C5
GO TO 214
213 A(I,J2)=2.*C6*C5
214 K=K+1
IF(K.EQ.NM1) GO TO 215
GO TO 103
215 K=1
L=L+1
GO TO 103
300 A(I,J4)=C8
A(I,J)=-C8-C7-(HC*DX)
A(I,N1)=-HC*TC*DX
IF(K.EQ.1) GO TO 301
A(I,J2)=C5*C6
IF(K.EQ.NM) GO TO 302
A(I,J1)=C5*C6
GO TO 303
301 A(I,J1)=2.*C5*C6
GO TO 303
302 A(I,J2)=2.*C5*C6
303 K=K+1
IF(K.EQ.NM1) GO TO 304
GO TO 103
304 K=1
L=L+1
103 CONTINUE
CALL STR(A)
STOP
END
```

```

SUBROUTINE STR(A)
  DIMENSION X(100),XX(100),A(100,101),ALPHA(100)
  COMMON N,DX,DY,P,DH,RO,RVC,NM,NM1,IREA
  1  FORMAT(15H NO CONVERGENCE)
  2  FORMAT(3HOL=,I3)
  3  FORMAT(1H0,10X,1HX,13X,1HJ,12X,5HALPHA/)
  4  FORMAT(3H      ,E16.8,4X,I3,5X,E16.8)
  5  FORMAT(8F10.4)
  6  FORMAT(4HOER=,1X,E16.8//)
  READ(1,5)(X(M),M=1,N)
  ER=9500.
  WRITE(3,6) ER
  KL=1
  LK=0
  N1=N+1
  L=0
  K=0
  BR=0.
  DO 801 I=1,N
801  ALPHA(I)=0.
203  DO 201 I=1,N
      IF(IREA.NE.1) GO TO 800
      BR=0.
      IF(I.EQ.1) KL=1
      ALPHA(I)=0.
      IF(I.EQ.1) LK=0
      LK=LK+1
      XP=-(ER/(X(I)+460.))
      DA=(RO*DY*P*EXP(XP))/(RVC*3600.)
      KM=I-NM
      IF(LK.EQ.NM1) GO TO 600
701  IF(KL.NE.1) GO TO 601
      ALPHA(I)=ALPHA(I)+DA
      GO TO 700
600  KL=KL+1
      LK=1
      GO TO 701
601  ALPHA(I)=ALPHA(I)+DA+ALPHA(KM)
700  IF(ALPHA(I).GE.1.) GO TO 800
      BR=EXP(XP)*DX*DY*P*DH*RO
800  SUM=A(I,N1)+BR
      DO 202 J=1,N
      IF(J.EQ.I) GO TO 202
      SUM=SUM-A(I,J)*X(J)
202  CONTINUE
      XX(I)=X(I)
      X(I)=SUM/A(I,I)
201  CONTINUE
      L=L+1
      K=K+1

```



```
IF(K.EQ.10) GO TO 204
IF(L.EQ.200) GO TO 500
207 DO 206 I=1,N
    B=X(I)-XX(I)
    B=ABS(B)
    IF(B.GT..1) GO TO 203
206 CONTINUE
    GO TO 501
204 K=0
    WRITE(3,2) L
    WRITE(3,3)
    DO 205 JK=1,N
205 WRITE(3,4) X(JK),JK,ALPHA(JK)
    GO TO 207
500 WRITE(3,1)
501 WRITE(3,2) L
    WRITE(3,3)
    DO 208 JK=1,N
208 WRITE(3,4) X(JK),JK,ALPHA(JK)
    RETURN
    END
```

APPENDIX B

Data Summary

I. 1 1/2 inch cylinder

1. Coolant: N₂

- A. Fuel flow rate: .88 cfm
- B. Free stream temperature: 1174°F
- C. Coolant reservoir temperature: 230°F
- D. Coolant flow rate: 20 scfh
- E. Blowing rate: .00583

θ(degrees)	0	15	30	60	90	105	120	150	180
Exterior surface Temperature (°F)	964	972	960	896	786	752	731	671	632
Interior Surface Temperature (°F)	877	888	871	820	735	756	722	671	632

2. Coolant: NH₃

- A. Fuel flow rate: .88 cfm
- B. Free stream temperature: 1174°F
- C. Coolant reservoir temperature: 163°F
- D. Coolant flow rate: 27 scfh
- E. Blowing rate: .00487
- F. Maximum dissociation (calculated): 25.9%

θ (degrees)	0	15	30	60	90	105	120	150	180
Interior Surface Temperature ($^{\circ}$ F)	917	900	905	816	726	675	653	597	597
Interior Surface Temperature ($^{\circ}$ F)	820	807	816	731	666	675	653	597	595

3. Coolant: NH_3

- A. Fuel flow rate: 1.08 cfm
- B. Free stream temperature: 1377 $^{\circ}$ F
- C. Coolant reservoir temperature: 169 $^{\circ}$ F
- D. Coolant flow rate: 27scfh
- E. Blowing rate: .00482
- F. Maximum dissociation (calculated): 72.5%

θ (degrees)	0	15	30	60	90	105	120	150	180
Exterior Surface Temperature ($^{\circ}$ F)	1162	--	1135	1005	891	--	823	754	720
Interior Surface Temperature ($^{\circ}$ F)	1053	--	1026	895	818	--	823	750	720

II. 1 Inch Cylinder

1. Coolant: NH_3

- A. Fuel flow rate: .88 cfm
- B. Free stream temperature: 1174 $^{\circ}$ F
- C. Coolant reservoir temperature: 195 $^{\circ}$ F
- D. Coolant flow rate: 27 scfh
- E. Blowing rate: .00776
- F. Maximum dissociation (calculated): 1.6%

θ (degrees)	0	45	90	135	180
--------------------	---	----	----	-----	-----

Interior Surface

Temperature ($^{\circ}$ F)	793	729	656	552	543
-----------------------------	-----	-----	-----	-----	-----

2. Coolant: NH_3

- A. Fuel flow rate: .88 cfm
- B. Free stream temperature: 1174° F
- C. Coolant reservoir temperature: 317° F
- D. Coolant flow rate: 18.4 scfh
- E. Blowing rate: .00533
- F. Maximum dissociation (calculated): 6.9%

θ (degrees)	0	45	90	135	180
--------------------	---	----	----	-----	-----

Interior Surface

Temperature ($^{\circ}$ F)	921	844	797	703	695
-----------------------------	-----	-----	-----	-----	-----

3. Coolant: NH_3

- A. Flue flow rate: .88 cfm
- B. Free stream temperature: 1174° F
- C. Coolant reservoir temperature: 360° F
- D. Coolant flow rate: 12.6 scfh
- E. Blowing rate: .00364
- F. Maximum dissociation (calculated): 16.4%

θ (degrees)	0	45	90	135	180
--------------------	---	----	----	-----	-----

Interior Surface

Temperature ($^{\circ}$ F)	1043	980	946	840	830
-----------------------------	------	-----	-----	-----	-----

ACKNOWLEDGEMENTS

I would like to express my appreciation to my advisor, Dr. R.L. Gorton for his supervision of the work that I did for this paper and for his invaluable assistance in its preparation.

Also, I would like to thank Joe Jenczmionka for his contribution to the design, construction, and operation of the experimental apparatus.

A special acknowledgement goes to my wife, Dorothy, for her patience and encouragement.

VITA

A. Warren Brecheisen II

Master of Science

Thesis: TRANSPIRATION COOLING OF TWO-DIMENSIONAL
 POROUS BODIES USING CHEMICALLY REACTING
 AND NONREACTING COOLANTS

Major Field: Mechanical Engineering

Biographical:

Personal Data: Born in Detroit, Michigan, December 4, 1944,
 the son of Adell W. and Jean E Brecheisen.

Education: Attended grade school in Garnett, Kansas; graduated
 from Garnett High School, Garnett, Kansas in 1962;
 attended Kansas State University, Manhattan, Kansas,
 from September, 1962, to May, 1969; received a Bachelor
 of Science degree in Mechanical Engineering from
 Kansas State University, Manhattan, Kansas, June, 1967;
 completed requirements for Master of Science degree
 in Mechanical Engineering in May, 1969.

Professional
Experience:

Was employed by the National Aeronautics and Space
Administration, Marshall Space Flight Center, Huntsville
Alabama, as an Engineering Coop Student from February,
1965, to June, 1965, and from February, 1966, to June,
1966; Was employed by Northrup Space Laboratories,
Huntsville, Alabama, as a Summer Engineer from June,
1965, to September, 1965; Was employed by Collins
Radio Company, Cedar Rapids, Iowa, as a Summer Engineer
from June, 1967, to September, 1967; Was employed by
Shell Oil Company, New Orleans, Louisiana, as a Summer
Engineer from June, 1968, to September, 1968; Was
employed by the Mechanical Engineering Department at
Kansas State University, Manhattan, Kansas, as a Graduate
Research Assistant from September, 1967, to June, 1968,
and from September, 1968, to June 1969.

TRANSPIRATION COOLING OF TWO-DIMENSIONAL
POROUS BODIES USING CHEMICALLY
REACTING AND NONREACTING
COOLANTS

by

ADELL WARREN BRECHEISEN II

B.S., Kansas State University, 1967

AN ABSTRACT OF A THESIS

submitted in partial fulfillment of the
requirements for the degree

MASTER OF SCIENCE

Department of Mechanical Engineering

KANSAS STATE UNIVERSITY
Manhattan, Kansas

1969

ABSTRACT

Transpiration cooling is an effective method of cooling structures which are receiving high convective heat fluxes. It has been shown that low molecular weight gases are more effective coolants, on a blowing rate basis, than are relatively high molecular weight gases. If a potential coolant undergoes an endothermic reaction in the temperature ranges of interest in transpiration cooling, that coolant has a much higher heat absorption capability than a nonreactive coolant with the same properties. If the reaction rate is proportional to temperature, the reactive coolant should also be able to reduce temperature gradients within the matrix. Ammonia is a potential reactive transpiration coolant. It undergoes a dissociation reaction, forming nitrogen and hydrogen, in the temperature ranges of interest.

A study was undertaken to compare the relative effectiveness of nitrogen, hydrogen, and ammonia when used to transpiration cool two-dimensional bodies receiving high convective heat fluxes from hot combustion gas streams. The study was done in two parts; analysis and experiment. For the analysis, a program was written to predict temperature profiles for a transpiration cooled, streamlined cylinder. Results from the analysis indicated that hydrogen, due to its low molecular weight, was the most effective coolant but also produced the largest temperature gradients in the wall. The results also indicated that ammonia could reduce matrix temperature gradients considerably.

The samples used in the experimental part of the study were porous

cylinders. The data obtained was insufficient to draw any conclusions about the relative effectiveness of the three coolants or the ability of ammonia to reduce temperature gradients. The samples all underwent thermal failure before enough data could be collected. The samples failed during ammonia runs. The cause of the failures was attributed to boundary layer combustion of the hydrogen produced by the dissociation of ammonia.